

1 **Continental-scale impacts of intra-seasonal rainfall variability**
2 **on simulated ecosystem responses in Africa**

3
4 Kaiyu Guan^{1,2*}, Stephen P. Good³, Kelly K. Caylor¹, Hisashi Sato⁴, Eric F. Wood¹, and
5 Haibin Li⁵

6
7 ¹Department of Civil and Environmental Engineering, Princeton University, Princeton,
8 NJ, USA

9 ²Department of Environmental & Earth System Science, Stanford University, Stanford,
10 CA 94025, USA

11 ³Department of Geology and Geophysics, University of Utah, Salt Lake City, UT
12 84112, USA

13 ⁴Graduate School of Environmental Studies, Nagoya University, D2-1(510) Furo-cho,
14 Chikusa-ku, Nagoya-city, Aichi 464-8601, Japan

15 ⁵Department of Earth and Planetary Sciences, Rutgers University, Piscataway, NJ
16 08854, USA

17
18 *Corresponding author:

19 Kaiyu Guan

20 Department of Environmental & Earth System Science,
21 Stanford University, Stanford, CA 94025, USA

22 Phone: 609-647-1368, Fax: 650-498-5099

23 Email: kaiyug@stanford.edu

24
25 Running title: Ecological Impacts of Intra-Seasonal Rainfall Variability

26
27 Submitted to *Biogeosciences*

28

29 **Abstract:**

30 Climate change is expected to change intra-seasonal rainfall variability, arising from
31 shifts in rainfall frequency, intensity and seasonality. These intra-seasonal changes are
32 likely to have important ecological impacts on terrestrial ecosystems. Yet, quantifying
33 these impacts across biomes and large climate gradients is largely missing. This gap
34 hinders our ability to better predict ecosystem services and their responses to climate
35 change, esp. for arid and semi-arid ecosystems. Here we use a synthetic weather
36 generator and an independently validated vegetation dynamic model (SEIB-DGVM)
37 to virtually conduct a series of “rainfall manipulation experiments” to study how
38 changes in the intra-seasonal rainfall variability affect continent-scale ecosystem
39 responses across Africa. We generated different rainfall scenarios with fixed total
40 annual rainfall but shifts in: i) frequency vs. intensity, ii) rainy season length vs.
41 frequency, iii) intensity vs. rainy season length. These scenarios were fed into
42 SEIB-DGVM to investigate changes in biome distributions and ecosystem
43 productivity. We find a loss of ecosystem productivity with increased rainfall
44 frequency and decreased intensity at very low rainfall regimes (<400 mm/year) and
45 low frequency (<0.3 event/day); beyond these very dry regimes, most ecosystems
46 benefit from increasing frequency and decreasing intensity, except in the wet tropics
47 (>1800 mm/year) where radiation limitation prevents further productivity gains. This
48 result reconciles seemingly contradictory findings in previous field studies on rainfall
49 frequency/intensity impacts on ecosystem productivity. We also find that changes in
50 rainy season length can yield more dramatic ecosystem responses compared with
51 similar percentage changes in rainfall frequency or intensity, with the largest impacts
52 in semi-arid woodlands. This study demonstrates that not all rainfall regimes are
53 ecologically equivalent, and that intra-seasonal rainfall characteristics play a
54 significant role in influencing ecosystem function and structure through controls on
55 ecohydrological processes. Our results also suggest that shifts in rainfall seasonality
56 have potentially large impacts on terrestrial ecosystems, and these understudied
57 impacts should be explicitly examined in future studies of climate impacts.

58 **Keywords:** rainfall frequency, rainfall intensity, rainfall seasonality, biome

59 distribution, Gross Primary Production (GPP), Africa

60

61 **1. Introduction**

62 Due to increased water holding capacity in the atmosphere as a consequence of global
63 warming (O’Gorman and Schneider, 2009), rainfall is projected to change in intensity
64 and frequency across much of the world (Easterling et al., 2000; Trenberth et al., 2003;
65 Chou et al., 2013), in conjunction with complex shifts in rainfall seasonality (Feng et
66 al., 2013; Seth et al., 2013). These changes possibly indicate a large increase in the
67 frequency of extreme events and variability in rainfall (Easterling et al., 2000; Allan
68 and Soden, 2008), and many of these changes may be accompanied with little changes
69 in total annual rainfall (Knapp et al., 2002; Franz et al., 2010). Meanwhile, regions
70 sharing similar mean climate state may have very different intra-seasonal variabilities,
71 and the ecological significance of intra-seasonal climate variabilities has been largely
72 overlooked previously in terrestrial biogeography (Good and Caylor, 2011). For
73 example, ecosystems in West Africa and Southwest Africa (Figure 1) share similar
74 total annual rainfall, but West Africa has much more intense rainfall events within a
75 much shorter rainy season, while Southwest Africa has a longer and less intense rainy
76 season. The same amount of total rainfall can come in very different ways, which may
77 cause distinctive ecosystem responses and structure. Understanding the impacts of
78 these regional differences in intra-seasonal rainfall variability and their possible future
79 changes on terrestrial ecosystems is critical for maintaining ecosystem services and
80 planning adaptation and mitigation strategies for ecological and social benefits
81 (Anderegg et al., 2013).

82

83 [insert Figure 1]

84

85 The changes in intra-seasonal rainfall characteristics, specifically frequency,
86 intensity and seasonality, have critical significance to ecosystem productivity and
87 structure (Porporato et al., 2001; Weltzin et al., 2003; Williams and Albertson, 2006;
88 Good and Caylor, 2011; Guan et al., 2014), but previous studies on this topic

89 (summarized in Table 1) have their limitations in the following aspects. First, existing
90 relevant field studies mostly focus on a single ecosystem, *i.e.* grasslands, and
91 subsequently only low rainfall regimes have been examined to date (mostly below
92 800mm/year, see Table 1). Grasslands have the largest sensitivity to hydrological
93 variabilities among all natural ecosystems (Scanlon et al., 2005; Guan et al., 2012),
94 however inferences drawn from a single ecosystem are limited in scope and difficult
95 to apply to other ecosystems. Second, even within grasslands, different studies have
96 seemingly contradictory findings (see Table 1), and there is a lack of a comprehensive
97 framework to resolve these inconsistencies. Specifically, whether increased rainfall
98 intensity with decreased rainfall frequency has positive (Knapp et al., 2002; Fay et al.,
99 2003; Robertson et al., 2009; Heisler-White et al., 2009) or negative impacts
100 (Heisler-White et al., 2009; Thomey et al., 2011) on grassland productivity is still
101 under debate. Third, previous relevant studies mostly focus on the impacts of rainfall
102 frequency and intensity (Table 1 and Rodríguez-Iturbe and Porporato, 2004), and
103 largely overlook the possible changes in rainfall seasonality. Rainfall frequency and
104 intensity mostly describe rainfall characteristics within the rainy season, but do not
105 account for the impacts of interplay between rainy season length and dry season
106 length (Guan et al., 2014). For ecosystems predominately controlled by water
107 availability, rainy season length constrains the temporal niche for active plant
108 physiological activities (van Schaik et al., 1993; Scholes and Archer, 1997), and large
109 variations in rainfall seasonality can lead to significant shifts in biome distribution
110 found from paleoclimate pollen records (e.g. Vincens et al., 2007). Given changes in
111 rainfall seasonality have been found in various tropical regions (Feng et al., 2013) and
112 have been projected in future climate (Biasutti and Sobel, 2009; Shongwe et al., 2009;
113 Seth et al., 2013), studies investigating their impacts on terrestrial ecosystems are
114 relatively rare, and very few field studies are designed to address this aspect (Table 1,
115 Bates et al., 2006; Svejcar et al., 2003; Chou et al., 2008). Finally, there is an
116 increasing trend of large-scale studies addressing rainfall variability and ecological
117 responses using satellite remote sensing (Fang et al., 2005; Zhang et al., 2005; Good
118 and Caylor, 2011; Zhang et al., 2013; Holmgren et al., 2013) and flux network data

119 (Ross et al., 2012). These large-scale studies are able to expand analyses to more
120 types of ecosystems and different climate conditions, and provide valuable
121 observation-based insights. However there are very few theoretical modeling works to
122 corroborate this effort. All these above issues call for a comprehensive modeling study
123 to investigate different aspects of intra-seasonal rainfall variability on terrestrial
124 ecosystems spanning large environmental gradients and various biomes.

125 In this paper, we aim to study ecological impacts of intra-seasonal rainfall
126 variability on terrestrial ecosystems. In particular, we design virtual “rainfall
127 manipulation experiments” to concurrently shift intra-seasonal rainfall characteristics
128 without changing total annual rainfall. We focus on the impacts of these different
129 rainfall scenarios on ecosystem productivity (e.g. Gross Primary Production, GPP)
130 and biome distributions in the African continent, simulated by an independently
131 validated dynamic vegetation model SEIB-DGVM (Sato and Ise, 2012). Previous
132 modeling approaches in this topic (Gerten et al., 2008; Hély et al., 2006) designed
133 various rainfall scenarios by rearranging (halving, doubling or shifting) the rainfall
134 amount based on the existing rainfall observations. In contrast to these approaches, we
135 design a weather generator based on a stochastic rainfall model (Rodríguez-Iturbe et
136 al., 1999), which allows us to implement a series of experiments by synthetically
137 varying two of the three rainfall characteristics (rainfall intensity, rainfall frequency,
138 and rainy season length) while fixing total annual rainfall at the current climatology.
139 We choose Africa as our test-bed mostly because the following two reasons: (1) the
140 rainfall regimes and biomes have large gradients varying from extremely dry
141 grasslands to highly humid tropical evergreen forests; (2) Africa is a continent usually
142 assumed to have few temperature constraints (Nemani et al., 2003), which will help to
143 isolate the impacts of precipitation from temperature, as one challenge in attributing
144 climatic controls on temperate ecosystems or Mediterranean ecosystems is the
145 superimposed influences from both temperature and precipitation. The overarching
146 science question we will address is: **How do African ecosystems respond to possible**
147 **changes in intra-seasonal rainfall variability (i.e. rainfall frequency, intensity and**
148 **rainy season length)?**

149

150 [insert Table 1]

151

152 **2. Materials and Methods**

153 **2.1 Methodology overview**

154 Table 1 summarizes previous field-based rainfall manipulation experiments, such as
155 the one that Knapp et al. (2002) did in a grassland that concurrently increasing rainfall
156 frequency and decreasing rainfall intensity while fixing total rainfall. The central idea
157 of our study is to design similar rainfall manipulation experiments but test them
158 virtually in the model domain across large environment gradients. We manipulate
159 rainfall changes through a weather generator based on a parsimonious stochastic
160 rainfall model (Rodriguez-Iturbe et al., 1984). We model the total amount of rainfall
161 during rainy season as a product of the three intra-seasonal rainfall characteristics for
162 the rainy season, rainfall frequency (λ , event/day), rainfall intensity (α , mm/event),
163 and rainy season length (T_w , days) (More details in section 2.3). Thus it is possible to
164 simultaneously perturb two of the rainfall characteristics away from their
165 climatological values while preserving the mean annual precipitation (MAP)
166 unchanged. We then feed these different rainfall scenarios into a well-validated
167 dynamic vegetation model (SEIB-DGVM, section 2.2) to study simulated ecosystem
168 responses. Detailed experiments design is described in section 2.5.

169

170 **2.2 SEIB-DGVM model and its performances in Africa**

171 We use a well-validated vegetation dynamic model SEIB-DGVM (Sato et al., 2007)
172 as the tool to study ecosystem responses to different rainfall variabilities. This model
173 follows the traditional “gap model” concept (Shugart, 1998) to explicitly simulate the
174 dynamics of ecosystem structure and function for individual plants at a set of virtual
175 vegetation patches, and uses results at these virtual patches as a surrogate to represent
176 large-scale ecosystem states. Thus individual trees are simulated from establishment,
177 competition with other plants, to death, which creates “gaps” for other plants to
178 occupy and develop. SEIB-DGVM includes mechanical-based and empirical-based

179 algorithms for land physical processes, plant physiological processes, and plant
180 dynamic processes. SEIB-DGVM contains algorithms that explicitly involve the
181 mechanisms of plant-related water stress (Figure 2; Sato and Ise, 2012). With similar
182 concepts to previous studies (e.g. Milly, 1992; Porporato et al., 2001), the current
183 SEIB-DGVM implements a continuous “water stress factor” (Equation 2) based on
184 the soil moisture status (Equation 1), scaling from 0 (most stressful) to 1 (with no
185 stress), which then acts to scale the stomatal conductance for plant transpiration and
186 carbon assimilation.

$$187 \quad stat_{water} = (S - S_w) / (S_f - S_w) \quad (\text{Equation 1})$$

$$188 \quad \text{Water stress factor} = 2 * stat_{water} - stat_{water}^2 \quad (\text{Equation 2})$$

189 where S , S_w and S_f refer to the fraction of volumetric soil water content within the
190 rooting depth, at the wilting point, and at field capacity, respectively. Figure 2
191 provides a schematic diagram of “water stress factor” from the SEIB-DGVM, and we
192 also include an approximated linear model that has been widely adopted elsewhere
193 (e.g. Milly, 1992; Porporato et al., 2001). The linear model uses an extra variable S^* ,
194 so called “critical point” of soil moisture: when $S > S^*$, there is no water stress (water
195 stress factor = 1); and when $S < S^*$, water stress factor linearly decreases with the
196 decrease of S . Though SEIB-DGVM adopts a quadratic form for “water stress factor”,
197 it essentially functions similarly as the linear model, such that S^* distinguishes two
198 soil moisture regimes that below which there is a large sensitivity of water stress to
199 soil moisture status, and above which there is little water stress. Understanding how
200 this “water stress factor” functions is the key to explain the following results.

201

202 [insert Figure 2]

203

204 SEIB-DGVM allows development of annual and perennial grasses as well as multiple
205 life cycles of grass at one year based on environmental conditions. Multiple life cycles
206 of tree growth per year are possible in theory but rarely happen in simulations (Sato
207 and Ise, 2012). Soil moisture status is the predominant factor to determine LAI of the
208 vegetation layer, which influences maximum daily productivity and leaf phenology.

209 When LAI exceeds 0 for 7 continuous days, dormant phase of perennial vegetation
210 layer changes into growth phase. While when LAI falls below 0 for 7 continuous days,
211 growth phase switches to dormant phase (Sato et al, 2007). SEIB-DGVM also
212 explicitly simulates light conditions and light competition among different PFTs in the
213 landscape based on its simulated 3D canopy structure and radiative transfer scheme
214 (Sato et al, 2007).

215 SEIB-DGVM has been tested both globally (Sato et al., 2007) and regionally for
216 various ecosystems (Sato et al., 2010; Sato, 2009; Sato and Ise, 2012), whose
217 simulated results compare favorably with ground observations and satellite remote
218 sensing measures for ecosystem composition, structure and function. In particular,
219 SEIB-DGVM has been successfully validated and demonstrated its ability in
220 simulating ecosystem structure and function in the African continent (Sato and Ise,
221 2012). Two plant function types (PFTs) of tropical woody species are simulated by
222 SEIB-DGVM in Africa: tropical evergreen trees and tropical deciduous trees. The
223 distribution of these two woody types in the simulation is largely determined by
224 hydro-climatic environments. Tropical evergreen trees only develop in regions where
225 water resources are sufficient all year around, so they can maintain leaves for all
226 seasons; otherwise, tropical deciduous trees could survive and dominate the landscape
227 as they can shed leaves if there is no sufficient water supply in its root zone during the
228 dry season (Sato and Ise, 2012). Trees and grasses coexist in a cell, with the floor of a
229 virtual forest monopolized by one of the two grass PFTs, C₃ or C₄ grass. The
230 dominating grass type is determined at the end of each year by air temperature,
231 precipitation, and CO₂ partial pressure (Sato and Ise, 2012).

232 SEIB-DGVM was run at 1 ° spatial resolution and at the daily step. It was spun-up
233 for 2000 years driven by the observed climate (1970-2000) repeatedly for the soil
234 carbon pool to reach steady state, followed by 200 years simulation driven by the
235 forcings based on the experiment design in Section 2.4. Because our purpose is to
236 understand the direct impacts of intra-seasonal rainfall variability, we turned off the
237 fire component of SEIB-DGVM to exclude fire-mediated feedbacks in the results.
238 Though we are fully aware of the important role of fire in interacting with rainfall

239 seasonality and their influence on African ecosystems (Bond et al., 2005; Lehmann et
240 al., 2011; Staver et al., 2012), studying these interactions is beyond the scope of this
241 work. For the similar reason, we fixed the atmospheric CO₂ concentration at 380
242 ppmv to exclude possible impacts of CO₂ fertilization effects.

243

244 **2.3 Synthetic weather generator**

245 The synthetic weather generator used here has two major components: i) to
246 stochastically generate daily rainfall based on a stochastic rainfall model, and ii) to
247 conditionally sample all other environmental variables from historical records to
248 preserve the covariance among climate forcing variables.

249 The stochastic rainfall model can be expressed as $MAP = \alpha \lambda T_w / f_w$, and we set f_w
250 to be 0.9, i.e. the period including 90% of total annual rainfall is defined as “rainy
251 season” (exchangeable with “wet season” hereafter). In particular, we first use
252 Markham (1970)’s approach to find the center of the rainy season, and then extend the
253 same length to both sides of the center until the total rainfall amount in this temporal
254 window (i.e. “rainy season”) is equal to 90% of the total annual rainfall. Rainy season
255 and dry season have their own rainfall frequency and intensity. Two seasons are
256 separately modeled based on the Market Poisson Process. Here we only focus on and
257 manipulate rainy-season rainfall characteristics in our study, as rainy-season rainfall
258 accounts for almost all the meaningful rainfall inputs for plant use. Thus in the
259 following paper, whenever we mention α or λ , we refer to those during the rainy
260 season.

261 In this rainfall model, any day can be either rainy or not, and a rainy day is
262 counted as one rainy event; rainfall events occur as a Poisson Process, with the
263 parameter $1/\lambda$ (unit: days/event) being the mean intervals between rainfall events, and
264 rainfall intensity α for each rainfall event following an exponential distribution, with α
265 being the mean rainfall intensity per event (Rodríguez-Iturbe et al., 1999). The wet
266 season length is modeled as a beta distribution bounded from 0 to 1, scaled by 365
267 days. All the necessary parameters to fit for the stochastic rainfall model (including
268 the mean and variance of rainfall frequency, intensity and length of wet and dry

269 seasons) were derived from the satellite-gauge-merged rainfall measurement from
270 TRMM 3b42V7 (Huffman et al., 2007) for the period of 1998 to 2012, based on the
271 above assumptions for the rainfall process. Specifically, we applied our definition of
272 “rainy season” to each year of the TRMM rainfall data for per pixel, and calculated
273 the mean and variance of the “rainy season length”, using which we fitted the beta
274 distribution for T_w . For rainfall frequency and intensity, we lumped all the wet or dry
275 season rainfall record together to derive their parameters. The two steps of the
276 synthetic weather generator are described below:

277 **Step 1:** Model the daily rainfall following the Marked Poisson process described
278 above. In particular, for a specific year, we first stochastically generate the wet season
279 length by sampling from the beta distribution, and the dry season length is determined
280 accordingly. Then we generate the daily rainfall for wet and dry season respectively.

281 **Step 2:** Based on the simulated daily rainfall time series in Step 1, we conditionally
282 sample temperature, wind, and humidity from the Global Meteorological Forcing
283 Dataset (GMFD, Sheffield et al., 2006), as well as cloud fraction and soil temperature
284 from the Climate Forecast System Reanalysis (CFSR) from National Centers for
285 Environmental Prediction (NCEP) (Saha et al., 2010). To sample for a specific day, all
286 the historical record within a 21-day time window centered at that specific day makes
287 up a sampling pool. From the sampling pool, we choose the day such that the
288 historical rainfall amount of the chosen day is within $(100-30)\%$ to $(100+30)\%$ of the
289 simulated daily rainfall amount. We then draw all the environmental variables (except
290 rainfall) on that sampled day to the new climate forcing. If we can find a sample from
291 the pool based on the above rule, this sampling is called “successful”. When there is
292 more than one suitable sample, we randomly select one. When there is no suitable
293 sample, we randomly select one day within the pool. The mean “successful” rate for
294 all the experiments and ensembles across Africa is 83%.

295 To test the validity of the synthetic weather generator, we ran SEIB-DGVM using
296 the historical climate record ($S_{\text{climatology}}$) and the synthetic forcing (S_{control}), with the
297 latter generated using the weather generator based on the rainfall characteristics
298 derived from the former. Figure S1 shows that the SEIB-DGVM simulations driven

299 by these two different forcings generate similar biome distributions with a Cohen's
300 Kappa coefficient of 0.78 (Cohen, 1960), and similar GPP patterns in Africa, with the
301 linear fit of annual GPP as: $GPP(S_{\text{control}}) = 1.03 \times GPP(S_{\text{climatology}}) + 0.215$ ($R^2=0.89$,
302 $P<0.0001$). Both biome and GPP patterns are consistent with observations (Sato and
303 Ise, 2012). These results provide confidence in using the synthetic weather generator
304 and SEIB-DGVM to conduct the further study.

305

306 **2.4 Experiment design**

307 Three experiments are designed as follows:

308 **Exp 1** (Perturbation of rainfall frequency and intensity, termed as $S_{\lambda-\alpha}$ hereafter)
309 Simulations forced by the synthetic forcings with varying λ and α simultaneously for
310 wet season (20% increases of λ and corresponding decreases of α to make MAP
311 unchanged; 20% decreases of λ and corresponding increases of α to make MAP
312 unchanged; no change for dry season rainfall characteristics), while fixing T_w at the
313 current climatology;

314 **Exp 2** (Perturbation of rainfall frequency and rainy season length, termed as $S_{T_w-\lambda}$)
315 Simulations forced by the synthetic forcing with varying T_w and λ simultaneously for
316 wet season (20% increases of T_w and corresponding decreases of λ to make MAP
317 unchanged; 20% decreases of T_w and corresponding increases of λ to make MAP
318 unchanged; no change for dry season characteristics), while fixing α at the current
319 climatology;

320 **Exp 3** (Perturbation of rainy season length and intensity, termed as $S_{T_w-\alpha}$) Simulations
321 forced by the synthetic forcing with varying T_w and α simultaneously for wet season
322 (20% increases of T_w and corresponding decreases of α to make MAP unchanged;
323 20% decreases of T_w and corresponding increases of α to make MAP unchanged; no
324 change for dry season characteristics), while fixing λ at the current climatology.

325 Because λ and T_w have bounded ranges ($\lambda \sim [0, 1]$ and $T_w \sim [0, 365]$), if these two
326 variables after perturbation exceeds the range, we would force their value to be the
327 lower or upper bound, and rearrange the other corresponding rainfall characteristic to
328 ensure MAP unchanged. Each rainfall scenario has six ensemble realizations of

329 synthetic climate forcings to account for the stochasticity of our synthetic weather
330 generator.

331

332 **3. Results**

333 We present the differences in simulated biome distributions of the three experiments
334 (i.e. $S_{\lambda-\alpha}$, $S_{TW-\lambda}$, $S_{TW-\alpha}$) in Figure 3, and their spatial patterns are shown in Figure S2
335 and S3. Differences in simulated annually averaged soil moisture and GPP for each
336 experiment are shown in Figure 4 and 6. These differences represent the simulated
337 ecosystem sensitivity to the slight perturbation of intra-seasonal rainfall characteristics
338 deviating from the current climatology. To further explore how MAP and these
339 rainfall characteristics affect the simulated GPP, Figure 5 shows the difference of
340 simulated GPP as a function of MAP and a perturbed rainfall characteristic in the
341 corresponding experiment. We term Figure 5 as “GPP sensitivity space”, and “positive
342 GPP sensitivity” means that GPP changes at the same direction with MAP or rainfall
343 characteristics, and vice versa for “negative GPP response”. These “GPP sensitivity
344 spaces” are generated based on the aggregated mean GPP in each bin of the rainfall
345 properties. The bin size for MAP, rainfall frequency, rainfall intensity and rainy
346 season length are 100 mm/year, 0.05 event/day, 1 mm/event and 15 days respectively.
347 We also provide the standard error (SE) of the “GPP sensitivity spaces” in each bin to
348 assess their uncertainties, with higher SE meaning larger uncertainties. $SE = \frac{\sigma}{\sqrt{n}}$,
349 where σ and n refer to the standard deviation of GPP values and the sample size in
350 each bin respectively. A series of illustrations in Figure 6 were generalized from the
351 simulated time series, and are used to explain the underlying mechanisms.

352

353 [insert Figure 3; Figure 4; Figure 5]

354

355 **3.1 Ecosystem sensitivity to rainfall frequency and intensity (Experiment $S_{\lambda-\alpha}$)**

356 Experiment $S_{\lambda-\alpha}$ assesses ecosystem responses after increasing rainfall frequency λ
357 and decreasing rainfall intensity α ($\lambda\uparrow$, $\alpha\downarrow$) under a fixed total annual rainfall. The

358 simulated biome distributions show that a small portion of regions are converted from
359 woodland to grassland at low rainfall regime (~500 mm/year), corresponding to a
360 decrease of GPP in these regions. In the high rainfall regime (around 1500 mm/year,
361 Figure 3a), increasing rainfall frequency significantly converts tropical evergreen
362 forests into woodlands. In the intermediate rainfall regime (600-1000 mm/year), there
363 is little change in biome distributions. We further check the spatial patterns of
364 differences in annual mean soil moisture and annual total GPP (Figure 4a and 5b). We
365 find that GPP increases with increasing rainfall frequency across most of the Africa
366 continent, except in the very dry end (in the southern and eastern Africa) and the very
367 wet regions (in central Africa and northeastern Madagascar). This GPP pattern mostly
368 mirrors the soil moisture change in woodlands and grasslands (Figure 4b), except the
369 wet tropics, where the changes of soil moisture and GPP are reversed.

370 Figure 5a shows the GPP sensitivity as a function of MAP and the climatological
371 rainfall frequency, and we find three major patterns:

372 **Pattern 1.1:** Negative GPP sensitivity shows up in the very dry end of MAP regime
373 (MAP<400 mm/year) and with relatively low rainfall frequency ($\lambda < 0.3$ event/day), i.e.
374 GPP decreases with more frequent but less intense rainfall in this low rainfall range.

375 **Pattern 1.2:** Across most rainfall ranges (MAP from 400 mm/year to 1600 mm/year),
376 increasing frequency of rainfall (and simultaneously decreasing rainfall intensity) lead
377 to positive GPP sensitivity. This positive GPP sensitivity peaks at the low range of
378 rainfall frequency (~0.35 event/day) and around the MAP of 1000 mm/year.

379 **Pattern 1.3:** At the high range of MAP (>1800 mm/year) with low rainfall frequency
380 (~0.4 event/day), GPP decreases with increased rainfall frequency.

381 The relationship of GPP sensitivity to MAP and rainfall intensity (Fig. 6c) has no
382 clear patterns as previous ones, mostly because the GPP sensitivity space (Fig. A4c)
383 contains large uncertainties (Fig. A4d, shown as large variance in the data). Thus we
384 will not over-interpret the pattern in Fig. 6c.

385 Pattern 1.1 and Pattern 1.2 can be explained by the illustrative time series in
386 Figure 6a and 6b, respectively. Figure 6a shows that when rainfall events are small
387 and very infrequent, increasing rainfall frequency while decreasing intensity would

388 cause more frequent downcrossings of soil moisture at the wilting point S_w , which
389 subsequently would reduce the effective time of carbon assimilation and plant growth
390 (i.e. when soil moisture is below S_w , plants would be in the extreme water stress and
391 slow down or stop physiological activity). This case only happens where MAP is very
392 low with low frequency and the biome is predominantly grasslands, which explains
393 why negative changes in soil moisture and GPP in Figure 4a and 4b are distributed in
394 those regions. This result also corroborates the field findings of the negative impacts
395 from increasing rainfall frequency in Heisler-White et al.(2009) and Thomey et al.
396 (2011) at low rainfall regimes.

397 Figure 6b provides the hydrological mechanism for the positive sensitivity of soil
398 moisture and GPP with increasing rainfall frequency over the most African continent
399 (Pattern 1.2). Once individual rainfall event has enough intensity and rainfall
400 frequency is enough, downcrossings of S_w would not easily happen. Instead, the
401 accumulative rainy-season soil moisture becomes the dominant control of plant
402 growth, and increasing rainfall frequency has led to a significant increase of soil
403 moisture for plant water use (Figure 4a and 4b). This conclusion drawn from our
404 numerical modeling is consistent with previous findings in Rodríguez-Iturbe and
405 Porporato (2004) based on stochastic modeling. We also find that this positive GPP
406 sensitivity reaches to its maximum in the intermediate total rainfall (~1000 mm/year)
407 and relatively low rainfall frequency (~0.35 event/day), indicating that in these
408 regimes increasing rainfall frequency could most effectively increase soil moisture for
409 plant water use and create marginal benefits of GPP to the increased rainfall frequency.
410 Further increase in large total annual rainfall or rainfall frequency would reduce the
411 sensitivity to water stress with fewer downcrossings of soil moisture critical point S^* ;
412 and once the soil moisture is always ample (i.e. above S^*), the changes in either MAP
413 or rainfall frequency would not alter plant water stress.

414 Pattern 1.3 also shows a negative GPP sensitivity, but its mechanism is different
415 from the previous case of Pattern 1.1. In regions with total rainfall usually more than
416 1800 mm/year, SEIB-simulated tropical forests exhibit radiation-limitation rather than
417 water-limitation during wet season. Increase of rainfall frequency at daily scale would

418 enhance cloud fraction and suppress plant productivity in these regions (Graham et al.,
419 2003). Thus even though soil moisture still increases (Figure 4a), GPP decreases with
420 increased rainfall frequency. This mechanism also explains why tropical evergreen
421 forests shrink its area with increased rainfall frequency (Figure 3a).

422 It is worth noting that the magnitude of GPP changes due to rainfall frequency
423 and intensity is relatively small in most of the woodlands, but can be relatively large
424 for drylands with MAP below 600 mm/year (up to 10-20% of annual GPP). This
425 pattern also explains why only modest changes in biome distribution happen between
426 woodlands and grasslands in $S_{\lambda-\alpha}$ (Figure 3a).

427

428 [insert Figure 6]

429

430 **3.2 Ecosystem sensitivity to rainfall seasonality and frequency (Experiment $S_{T_w-\lambda}$)**

431 Experiment $S_{T_w-\lambda}$ assesses ecosystem responses after increasing rainy season length
432 and decreasing rainfall frequency (i.e. $T_w \uparrow$, $\lambda \downarrow$) under a fixed total annual rainfall. The
433 simulated biome distribution shows a gain of area in tropical evergreen forests
434 converted from woodlands. The northern Africa has an area increase of woodlands
435 converted from grasslands, and African Horn region has a small expansion of
436 grasslands into woodlands (Figure 3b). Figure 4c and 4d show that increasing rainy
437 season length T_w and decreasing frequency λ would significantly increase annual
438 mean soil moisture and GPP (up to 30%) in most woodland area. Meanwhile
439 decreased soil moisture and GPP are found in the southern and eastern Africa.
440 Tropical evergreen forests show little response. We further explore the GPP sensitivity
441 space in Figure 5e and 5g, and find the following robust patterns (based on small
442 standard errors shown in Figure 5f and 5h):

443 **Pattern 2.1:** The negative GPP sensitivity tends to happen where MAP is mostly
444 below 1000 mm/year with long rainy season length ($T_w > 150$ days) and low rainfall
445 frequency ($\lambda < 0.35$ event/day).

446 **Pattern 2.2:** When MAP and rainfall frequency are large enough (MAP > 1000
447 mm/year and $\lambda > 0.4$ event/day), decreasing λ while increasing T_w would significantly

448 increase GPP. The maximum positive GPP sensitivity happens at the intermediate
449 MAP range (1100-1500 mm/year) and the high rainfall frequency ($\lambda \sim 0.7$ event/day).

450 **Pattern 2.3:** There exists an “optimal rainy season length” for relative changes in
451 ecosystem productivity across large MAP ranges (the white area between the red and
452 blue space in Figure 5e). For the same MAP, any deviation of T_w from the “optimal
453 rainy season length” would reduce GPP. This “optimal rainy season length” follows
454 an increasing trend with MAP until 1400 mm/year.

455 Figure 6c explains the hydrological mechanism for the negative GPP sensitivity
456 in Pattern 2.1. In the situation with low MAP and infrequent rainfall events,
457 decreasing rainfall frequency and expanding rainy season length (i.e. $T_w \uparrow$, $\lambda \downarrow$) would
458 lead to longer intervals between rainfall events and possibly longer excursions below
459 S_w , which would disrupt continuous plant growth and have detrimental effects on
460 ecosystem productivity. It is worth noting that long rainy season in dryland (Figure 5e)
461 is usually accompanied with low rainfall frequency (Figure 5g). The southern African
462 drylands (south of 15 °S) typically fall in this category, and these regions thus have
463 negative GPP sensitivity (Figure 4c and 4d), accompanied by a small biome
464 conversion from woodlands to grasslands (Figure 3b).

465 Figure 6d explains the hydrological mechanisms for the positive GPP sensitivity
466 in Pattern 2.2. When rainfall is ample enough to maintain little or no water stress
467 during rainy season, increasing the interval of rainfall events may introduce little
468 additional water stress but can significantly extend the growing season. This situation
469 mostly happens in woodlands, where limited water stress exists during rainy season,
470 and dry season length is the major constraint for plant growth. Thus the increase of
471 rainy season length extends the temporal niche for plant growth, and leads to a
472 significant woodland expansion to grasslands as well as an expansion of tropical
473 evergreen forests to woodlands (Figure 3b).

474 The little GPP sensitivity in tropical evergreen forest regions is mostly attributed
475 to the long rainy season length in this ecosystem. Thus further increasing T_w may
476 reach to its saturation (365 days) and has little impact to ecosystem productivity. This
477 also explains why the magnitude of GPP sensitivity is much smaller at high MAP

478 range than at the intermediate MAP range.

479 The finding of “optimal rainy season length” across different rainfall regimes
480 (Figure 5e) is consistent with our previous empirical finding about the similar pattern
481 of “optimal rainy season length” for tree fractional cover in Africa derived based on a
482 satellite remote sensing product (Guan et al., 2014). The existence of “optimal rainy
483 season length” fully demonstrates the importance to explicitly consider the non-linear
484 impacts of rainy season length on ecosystem productivity under climate change,
485 which has been largely overlooked before.

486

487 **3.3 Ecosystem sensitivity to rainfall seasonality and intensity ($S_{TW-\alpha}$)**

488 Results of Experiment $S_{TW-\alpha}$ have many similarities with those of $S_{TW-\lambda}$, including the
489 similar changes in biome distributions (Figure 3), soil moisture and GPP patterns
490 (Figure 4e and 4f). We further find that the GPP sensitivity space with MAP and rainy
491 season length for $S_{TW-\alpha}$ (Figure 5i) is also similar with that for $S_{TW-\lambda}$ (Figure 5e). One
492 new finding is that rainfall intensity has little impact on GPP, as the contour lines in
493 Figure 5k are mostly parallel with y-axis (i.e. rainfall intensity).

494 Figure 6e and 6f explain the governing hydrological mechanisms for the patterns
495 of $S_{TW-\alpha}$, which also have many similarities with $S_{TW-\lambda}$. For the negative case (Figure
496 6e), decreasing rainfall intensity and increasing rainy season length in the very low
497 MAP regime may lead to more downcrossings of S_w and interrupt continuous plant
498 growth. The positive case (Figure 6e) is similar as that in Figure 6d, i.e. the
499 repartitioning of excessive wet-season rainfall to the dry season for an extended
500 growing period would significantly benefit plant growth and possible increase tree
501 fraction cover.

502

503 **4. Discussion**

504 In this paper we provide a new modeling approach to systematically interpret the
505 ecological impacts from changes in intra-seasonal rainfall characteristics (i.e. rainfall
506 frequency, rainfall intensity and rainy season length) across biomes and climate
507 gradients in the African continent.

508

509 **4.1 Limitation of the methodology**

510 Though our modeling framework is able to characterize the diverse ecosystem
511 responses to the shifts in different rainfall characteristics, it nevertheless has its
512 limitations. The current rainfall model only deals with the case of single rainy season
513 per year, and approximates the case of double rainy seasons per year to be the single
514 rainy season case. This assumption may induce unrealistic synthetic rainfall patterns
515 in the equatorial dryland regions, in particular the Horn of Africa. Thus the simulated
516 sensitivity of these regions may be less reliable. We also assume that rainfall
517 frequency and intensity are homogenous throughout wet seasons (or dry seasons), but
518 in reality they have seasonal variations. We only consider rainy season length for
519 rainfall seasonality, and neglect the possible temporal phase change; in reality, rainfall
520 seasonality change usually has length and phase shifts in concert. These
521 rainfall-model-related limitations can be possibly overcome by simulating smaller
522 intervals of rainfall processes (e.g. each month has their own α and λ) rather than
523 simulating the whole wet or dry season using one fixed set of α and λ . Besides, only
524 using one ecosystem model also means that the simulated ecosystem sensitivity can
525 be model-specific. Though magnitudes or thresholds for the corresponding patterns
526 may vary depending on different models, we argue that the qualitative results for the
527 GPP sensitivity patterns (e.g. Figure 4 and Figure 5) should hold as the necessary
528 ecohydrological processes have been incorporated in SEIB-DGVM. We also
529 recognize that to exclude fire impacts in the current simulation may bring some
530 limitation for this study, as evidence shows that many savanna regions can be bistable
531 due to fire effects (Staver et al 2011; Hirota et al 2011; Higgins and Scheiter 2012;
532 also see for a possible rebuttal in Hanan et al, 2013). Changes in rainfall regimes not
533 only have direct effects on vegetation productivity, but can also indirectly affect
534 ecosystems through its interactions with fire, with rapid biome shifts being a possible
535 consequence. These feedbacks can be important in situations when the changes in
536 growing season length are related to fuel loads, fuel moisture dynamics and hence fire
537 intensity (Lehmann et al., 2011). Quantifying these fire-rainfall feedbacks will be the

538 important future direction to pursue.

539

540 **4.2 Clarifying the impacts of rainfall frequency and intensity on ecosystem** 541 **productivity**

542 In this modeling study, we provide a plausible answer to possibly resolve the previous
543 debate about whether increasing rainfall intensity (or equivalently decreasing rainfall
544 frequency, i.e. $\lambda \downarrow$, $\alpha \uparrow$) has positive or negative impacts on above-ground primary
545 productivity under a fixed annual rainfall total. We identify that negative GPP
546 sensitivity with increased rainfall frequency is possible at very low MAP range (~ 400
547 mm/year) with relatively low rainfall frequency (<0.35 event/day) (Figure 5a), due to
548 the increased downcrossings of soil moisture wilting point, which restricts plant
549 growth (Figure 6a). This derived MAP threshold (~400 mm/year) is consistent with
550 our meta-analysis based on the previous field studies (Table 1), which shows a
551 threshold of MAP at 340 mm/year separates positive and negative impacts of more
552 intense rainfall on aboveground net primary production (ANPP). Our findings are also
553 consistent with another study about increased tree encroachments with increased
554 rainfall intensity in low rainfall regime (<544mm/year, Kulmatiski and Beard, 2013),
555 which essentially follows the same mechanism as identified in Figure 6a.

556 In addition, we thoroughly investigated the ecosystem responses across a wide
557 range of annual rainfall in Africa. We find that beyond the very low rainfall range
558 (below 400 mm/year), most grasslands and woodlands would benefit from increasing
559 rainfall frequency, which also corroborate the previous large-scale findings about the
560 positive effects of increased rainfall frequency (and decreased rainfall intensity) for
561 tree fractions across the African continent (Good and Caylor, 2011). The only
562 exception happens at the very wet end of MAP (~1800mm/year) where cloud-induced
563 radiation-limitation may suppress ecosystem productivity with increased rainfall
564 frequency. We also find that changes in rainfall frequency and intensity mostly affect
565 grassland-dominated savannas (changes of GPP up to 20%), and the corresponding
566 effects are much smaller in woodlands and have little impact on woodland distribution.
567 Though this work is only based on a single model, it provides a primary assessment

568 for understanding of interactive changes between λ and α in ecosystem functioning,
569 and expands the analysis to a wide range of annual rainfall conditions compared with
570 previous studies (e.g. Porporato et al., 2004).

571

572 **4.3 Ecological importance of rainy season length**

573 The results involving rainy season length (i.e. $S_{T_w-\lambda}$ and $S_{T_w-\alpha}$) provide evidence for
574 the ecological importance of rainfall seasonality. The magnitudes of changes in soil
575 moisture, GPP and biome distribution in $S_{T_w-\lambda}$ and $S_{T_w-\alpha}$ are much larger than those of
576 $S_{\lambda-\alpha}$, with almost one order of magnitude difference. These disproportional impacts of
577 T_w indicate that slight changes in rainy season length could modify biome distribution
578 and ecosystem function more dramatically compared with the same percentage
579 changes in rainfall frequency and intensity. We also notice that $S_{T_w-\lambda}$ and $S_{T_w-\alpha}$ have
580 similar results. This is because that both λ and α describe rainfall characteristics
581 within wet season, while T_w describes rainfall characteristics of both dry season and
582 wet season. Cautions are required that our simplified treatment rainy season length
583 may overestimate its importance, and we did not consider the rainfall phase
584 information here.

585 Given the importance of rainy season length, its ecological impacts under climate
586 change are largely understudied, though substantial shifts in rainfall seasonality have
587 been projected in both Sahel and South Africa (Biasutti and Sobel, 2009; Shongwe et
588 al., 2009; Seth et al., 2013). Here we only address the rainfall seasonality in terms of
589 its length, and future changes in rainfall seasonality may modify their phase and
590 magnitude in concert. The climate community has focused on the increase of extreme
591 rainfall events (Field et al., 2012), which could be captured by the changes in λ or α
592 towards heavier tails in their distribution. However, explicit and systematic
593 assessments and projection on rainfall seasonality changes (including both phase and
594 magnitude) are still limited even in the latest Intergovernmental Panel on Climate
595 Change (IPCC) synthesis reports (Field et al., 2012; Stocker et al., 2013). More
596 detailed studies related to these changes and their ecological implications are required
597 for future hydroclimate-ecosystem research.

598

599 **4.4 Not all rainfall regimes are ecologically equivalent**

600 As Figure 1 gives a convincing example that the same total annual rainfall may arrive
601 in a very different way, our results further demonstrate that ecosystems respond
602 differently to the changes in these intra-seasonal rainfall variability. For example, with
603 similar MAP, drylands in West Africa and Southwest Africa show reversed responses
604 to the same changes in intra-seasonal rainfall variability. As shown in the experiments
605 of $S_{T_w-\lambda}$ and $S_{T_w-\alpha}$, increasing T_w while decreasing λ or α generates slightly positive
606 soil moisture and GPP sensitivity in West Africa (Figure 4c and 4d), but would cause
607 relatively large GPP decrease in Southwest Africa. The prior hydroclimate conditions
608 of these two regions can explain these differences: West Africa has much shorter rainy
609 season with more intense rainfall events; in contrast, Southwest Africa has a long
610 rainy season but many small and sporadic rainfall events. As a result, under a fixed
611 annual rainfall total, slightly increasing rainy season and meanwhile decreasing
612 rainfall intensity would benefit plant growth in West Africa, but the same change
613 would lengthen dry spells in Southwest Africa and bring negative effects to the
614 ecosystem productivity. We further deduce that the rainfall use efficiency (RUE,
615 defined as the ratio of plant net primary production to total rainfall amount) in these
616 two drylands could be different: West Africa may have lower RUE, and the intense
617 rainfall could lead to more infiltration-excess runoff, and thus less water would be
618 used by plants; while Southwest Africa can have higher RUE, because its sporadic
619 and feeble rainfall events would favor grass to fully take the advantage of the
620 ephemerally existed water resources. This conclusion is partly supported by Martiny
621 et al. (2007) based on satellite remote sensing. We further hypothesize that landscape
622 geomorphology in these two drylands may be different and therefore reflect
623 distinctive rainfall characteristics. More bare soil may exist in West Africa grasslands
624 due to intense-rainfall-induced erosion, while Southwest Africa may have more grass
625 fraction and less bare soil fraction. Testing these interesting hypotheses is beyond the
626 scope of this paper, but is worthy the further exploration.

627

628

629 **Acknowledgements:**

630 K. Guan and E. F. Wood acknowledge the financial supports from the NASA NESSF
631 fellowship. S.P. Good and K. K. Caylor acknowledge the financial supports from the
632 National Science Foundation through the Grant EAR-0847368. The authors thank
633 Ignacio Rodríguez-Iturbe for his valuable inputs and discussion.

634

635

636 **References:**

- 637 Anderegg, L. D. L.; Anderegg, W. R. L. & Berry, J. A. (2013), 'Not all droughts are
638 created equal: translating meteorological drought into woody plant mortality', *Tree*
639 *Physiology* **33**, 701-712.
- 640
- 641 Bates, J.; Svejcar, T.; Miller, R. & Angell, R. (2006), 'The effects of precipitation
642 timing on sagebrush steppe vegetation', *Journal of Arid Environments* **64**, 670-697.
- 643
- 644 Biasutti, M. & Sobel, A. H. (2009), 'Delayed Sahel rainfall and global seasonal cycle in
645 a warmer climate', *Geophysical Research Letters* **36**, L23707.
- 646
- 647 Bond, W. J.; Woodward, F. I. & Midgley, G. F. (2005), 'The Global Distribution of
648 Ecosystems in a World without Fire', *New Phytologist* **165**(2), 525-537.
- 649
- 650 Easterling, D. R.; Meehl, G. A.; Parmesan, C.; Changnon, S. A.; Karl, T. R. & Mearns,
651 L. O. (2000), 'Climate Extremes: Observations, Modeling, and Impacts', *Science* **289**,
652 2068-2074.
- 653
- 654 Fang, J.; Piao, S.; Zhou, L.; He, J.; Wei, F.; Myneni, R. B.; Tucker, C. J. & Tan, K.
655 (2005), 'Precipitation patterns alter growth of temperate vegetation', *Geophysical*
656 *Research Letters* **32**, L21411.
- 657
- 658 Fay, P. A.; Carlisle, J. D.; Knapp, A. K.; Blair, J. M. & Collins, S. L. (2003),
659 'Productivity responses to altered rainfall patterns in a C4-dominated grassland',
660 *Oecologia* **137**, 245-251.
- 661
- 662 Feng, X.; Porporato, A. & Rodriguez-Iturbe, I. (2013), 'Changes in rainfall seasonality
663 in the tropics', *Nature Climate Change*.
- 664
- 665 Field, C.; Barros, V.; Stocker, T.; Qin, D.; Dokken, D.; Ebi, K.; Mastrandrea, M.; Mach,
666 K.; Plattner, G.-K.; Allen, S.; Tignor, M. & Midgley, P., ed. (2012), *IPCC, 2012:
667 Managing the Risks of Extreme Events and Disasters to Advance Climate Change
668 Adaptation. A Special Report of Working Groups I and II of the Intergovernmental
669 Panel on Climate Change*, Cambridge University Press, Cambridge, UK, and New
670 York, NY, USA.
- 671
- 672 Franz, T. E.; Caylor, K. K.; Nordbotten, J. M.; Rodríguez-Iturbe, I. & Celia, M. A.
673 (2010), 'An ecohydrological approach to predicting regional woody species distribution
674 patterns in dryland ecosystems', *Advances in Water Resources* **33**(2), 215-230.
- 675
- 676 Gerten, D.; Luo, Y.; Maire, G. L.; Parton, W. J.; Keough, C.; Weng, E.; Beier, C.; Ciais,
677 P.; Cramer, W.; Dukes, J. S.; Hanson, P. J.; Knapp, A. A. K.; Linder, S.; Nepstad, D.;
678 Rustad, L. & Sowerby, A. (2008), 'Modelled effects of precipitation on ecosystem
679 carbon and water dynamics in different climatic zones', *Global Change Biology* **14**,

680 2365-2379.

681

682 Good, S. P. & Caylor, K. K. (2011), 'Climatological determinants of woody cover in
683 Africa', *Proceedings of the National Academy of Sciences of United States of America*
684 **108(12)**, 4902-4907.

685

686 Graham, E. A.; Mulkey, S. S.; Kitajima, K.; Phillips, N. G. & Wright, S. J. (2003),
687 'Cloud cover limits net CO₂ uptake and growth of a rainforest tree during tropical
688 rainy seasons', *Proceedings of the National Academy of Sciences of the United States*
689 *of America* **100(2)**, 572-576.

690

691 Guan, K.; Wood, E. F. & Caylor, K. K. (2012), 'Multi-sensor derivation of regional
692 vegetation fractional cover in Africa', *Remote Sensing of Environment* **124**, 653-665.

693

694 Guan, K.; Wood, E. F.; Medvigy, D.; Pan, M.; Caylor, K. K.; Sheffield, J.; Kimball, J.;
695 Xu, X. & Jones, M. O. (2014), 'Terrestrial hydrological controls on vegetation
696 phenology of African savannas and woodlands', *Journal of Geophysical Research*.

697

698 Hanan, N. P.; Tredennick, A. T.; Prihodko, L.; Bucini, G. & Dohn, J. (2013), 'Analysis
699 of stable states in global savannas: is the CART pulling the horse?', *Global Ecology and*
700 *Biogeography* **23(3)**, 259-263.

701

702 Harper, C. W.; Blair, J. M.; Fay, P. A.; Knapp, A. K. & Carlisle, J. D. (2005), 'Increased
703 rainfall variability and reduced rainfall amount decreases soil CO₂ flux in a grassland
704 ecosystem', *Global Change Biology* **11**, 322-334.

705

706 Heisler-White, J. L.; Blair, J. M.; Kelly, E. F.; Harmoney, K. & Knapp, A. K. (2009),
707 'Contingent productivity responses to more extreme rainfall regimes across a grassland
708 biome', *Global Change Biology* **15(12)**, 2894-2904.

709

710 Hély, C.; Bremond, L.; Alleaume, S.; Smith, B.; Sykes, M. T. & Guiot, J. (2006),
711 'Sensitivity of African biomes to changes in the precipitation regime', *Global Ecology*
712 *and Biogeography* **15**, 258-270.

713

714 Hirota, M.; Holmgren, M.; Nes, E. H. V. & Scheffer, M. (2011), 'Global Resilience of
715 Tropical Forest and Savanna to Critical Transitions', *Science* **334**, 232-235.

716

717 Higgins, S. I. & Scheiter, S. (2012), 'Atmospheric CO₂ forces abrupt vegetation shifts
718 locally, but not globally', *Nature* **488**, 209-212.

719

720 Holmgren, M.; Hirota, M.; van Nes, E. H. & Scheffer, M. (2013), 'Effects of
721 interannual climate variability on tropical tree cover', *Nature Climate Change*.

722

723 Huffman, G. J.; Bolvin, D. T.; Nelkin, E. J.; Wolff, D. B.; Adler, R. F.; Bowman, K. P.

724 & Stocker, E. F. (2007), 'The TRMM Multisatellite Precipitation Analysis (TMPA):
725 Quasi-Global, Multiyear, Combined-Sensor Precipitation Estimates at Fine Scales',
726 *Journal of Hydrometeorology* **8**, 38-55.
727

728 Knapp, A. K.; Fay, P. A.; Blair, J. M.; Collins, S. L.; Smith, M. D.; Carlisle, J. D.;
729 Harper, C. W.; Danner, B. T.; Lett, M. S. & McCarron, J. K. (2002), 'Rainfall
730 Variability, Carbon Cycling, and Plant Species Diversity in a Mesic Grassland', *Science*
731 **298**, 2202-2205.
732

733 Kulmatiski, A. & Beard, K. H. (2013), 'Woody plant encroachment facilitated by
734 increased precipitation intensity', *Nature Climate Change*.
735

736 Lehmann, C. E. R.; Archibald, S. A.; Hoffmann, W. A. & Bond, W. J. (2011),
737 'Deciphering the distribution of the savanna biome', *New Phytologist* **191**, 197-209.
738

739 Markham, C. (1970), 'Seasonality of precipitation in the United States', *Annals of the*
740 *Association of American Geographers* **60(3)**, 593-597.
741

742 Martiny, N.; Camberlin, P.; Richard, Y. & Philippon, N. (2006), 'Compared regimes of
743 NDVI and rainfall in semi-arid regions of Africa', *International Journal of Remote*
744 *Sensing* **27(23)**, 5201-5223.
745

746 Miranda, J.; Armas, C.; Padilla, F. & Pugnaire, F. (2011), 'Climatic change and rainfall
747 patterns: Effects on semi-arid plant communities of the Iberian Southeast', *Journal of*
748 *Arid Environments* **75**, 1302-1309.
749

750 Nemani, R. R.; Keeling, C. D.; Hashimoto, H.; Jolly, W. M.; Piper, S. C.; Tucker, C. J.;
751 Myneni, R. B. & Running, S. W. (2003), 'Climate-Driven Increases in Global
752 Terrestrial Net Primary Production from 1982 to 1999', *Science* **300**, 1560-1563.
753

754 O'Gorman, P. A. & Schneider, T. (2009), 'The physical basis for increases in
755 precipitation extremes in simulations of 21st-century climate change', *Proceedings of*
756 *the National Academy of Sciences of the United States of America* **106(35)**,
757 14773-14777.
758

759 Porporato, A.; Daly, E. & Rodríguez-Iturbe, I. (2004), 'Soil Water Balance and
760 Ecosystem Response to Climate Change', *American Naturalist* **164(5)**, 625-632.
761

762 Porporato, A.; Laio, F.; Ridolfi, L. & Rodríguez-Iturbe, I. (2001), 'Plants in
763 water-controlled ecosystems: active role in hydrologic processes and response to water
764 stress - III. Vegetation water stress', *Advances in Water Resources* **24(7)**, 725-744.
765

766 Robertson, T. R.; Bell, C. W.; Zak, J. C. & Tissue, D. T. (2009), 'Precipitation timing
767 and magnitude differentially affect aboveground annual net primary productivity in

768 three perennial species in a Chihuahuan Desert grassland', *New Phytologist* **181**,
769 230-242.
770

771 Rodr íguez-Iturbe, I.; Gupta, V. K. & Waymire, E. (1984), 'Scale Considerations in the
772 Modeling of Temporal Rainfall', *Water Resource Research* **20(11)**, 1611-1619.
773

774 Rodr íguez-Iturbe, I. & Porporato, A. (2004), *Ecohydrology of Water-Controlled*
775 *Ecosystems: Soil Moisture And Plant Dynamics*, Cambridge University Press.
776

777 Rodr íguez-Iturbe, I.; Porporato, A.; Ridolfi, L.; Isham, V. & Cox, D. R. (1999),
778 'Probabilistic Modelling of Water Balance at a Point: The Role of Climate, Soil and
779 Vegetation', *Proceedings: Mathematical, Physical and Engineering Sciences* **455**,
780 3789-3805.
781

782 Ross, I.; Misson, L.; Rambal, S.; Arneth, A.; Scott, R. L.; Carrara, A.; Cescatti, A. &
783 Genesio, L. (2012), 'How do variations in the temporal distribution of rainfall events
784 affect ecosystem fluxes in seasonally water-limited Northern Hemisphere shrublands
785 and forests?', *Biogeosciences* **9**, 1007-1024.
786

787 Saha, S.; Moorthi, S.; Pan, H.-L.; Wu, X.; Wang, J.; Nadiga, S.; Tripp, P.; Kistler, R.;
788 Woollen, J.; Behringer, D.; Liu, H.; Stokes, D.; Grumbine, R.; Gayno, G.; Wang, J.;
789 Hou, Y.-T.; Chuang, H.-Y.; Juang, H.-M. H.; Sela, J.; Iredell, M.; Treadon, R.; Kleist,
790 D.; Delst, P. V.; Keyser, D.; Derber, J.; Ek, M.; Meng, J.; Wei, H.; Yang, R.; Lord, S.;
791 Dool, H. V. D.; Kumar, A.; Wang, W.; Long, C.; Chelliah, M.; Feng, Y.; Huang, B.;
792 Schemm, J.-K.; Ebisuzaki, W.; Lin, R.; Xie, P.; Chen, M.; Zhou, S.; Higgins, W.; Zou,
793 C.-Z.; Liu, Q.; Chen, Y.; Han, Y.; Cucurull, L.; Reynolds, R. W.; Rutledge, G. &
794 Goldberg, M. (2010), 'The NCEP Climate Forecast System Reanalysis', *Bulletin of the*
795 *American Meteorological Society* **91**, 1015-1057.
796

797 Sato, H. (2009), 'Simulation of the vegetation structure and function in a Malaysian
798 tropical rain forest using the individual-based dynamic vegetation model SEIB-DGVM',
799 *Forest Ecology and Management* **257**, 2277-2286.
800

801 Sato, H. & Ise, T. (2012), 'Effect of plant dynamic processes on African vegetation
802 responses to climate change: analysis using the spatially explicit individual-based
803 dynamic global vegetation model (SEIB-DGVM)', *Journal of Geophysical Research*
804 **117**, G03017.
805

806 Sato, H.; Itoh, A. & Kohyama, T. (2007), 'SEIB-DGVM: A new Dynamic Global
807 Vegetation Model using a spatially explicit individual-based approach', *Ecological*
808 *Modelling* **200(3-4)**, 279-307.
809

810 Sato, H.; Kobayashi, H. & Delbart, N. (2010), 'Simulation study of the vegetation
811 structure and function in eastern Siberian larch forests using the individual-based

812 vegetation model SEIB-DGVM', *Forest Ecology and Management* **259**, 301-311.

813

814 Scanlon, T. M.; Caylor, K. K.; Manfreda, S.; Levin, S. A. & Rodriguez-Iturbe, I. (2005),
815 'Dynamic response of grass cover to rainfall variability: implications for the function
816 and persistence of savanna ecosystems', *Advances in Water Resources* **28**, 291-302.

817

818 Shugart, H. H. (1998), 'Terrestrial ecosystems in changing environments', Cambridge
819 University Press, United Kingdom.

820

821 van Schaik, C. P.; Terborgh, J. W. & Wright, S. J. (1993), 'The Phenology of Tropical
822 Forests: Adaptive Significance and Consequences for Primary Consumers', *Annual
823 Review of Ecology and Systematics* **24**, 353-377.

824

825 Scholes, R. J. & Archer, S. R. (1997), 'Tree-Grass Interactions in Savannas', *Annual
826 Review of Ecology and Systematics* **28**, 517-544.

827

828 Seth, A.; Rauscher, S. A.; Biasutti, M.; Giannini, A.; Camargo, S. J. & Rojas, M. (2013),
829 'CMIP5 Projected Changes in the Annual Cycle of Precipitation in Monsoon Regions',
830 *Journal of Climate* **26**, 7328-7351.

831

832 Sheffield, J.; Goteti, G. & Wood, E. F. (2006), 'Development of a 50-Year
833 High-Resolution Global Dataset of Meteorological Forcings for Land Surface
834 Modeling', *Journal of Climate* **19**, 3088-3111.

835

836 Shongwe, M. E.; van Oldenborgh, G. J.; van den Hurk, B. J. J. M.; de Boer, B.; Coelho,
837 C. A. S. & van Aalst, M. K. (2009), 'Projected Changes in Mean and Extreme
838 Precipitation in Africa under Global Warming. Part I: Southern Africa', *Journal of
839 Climate* **22**, 3819-3837.

840

841 Staver, A. C.; Archibald, S. & Levin, S. A. (2011), 'The Global Extent and
842 Determinants of Savanna and Forest as Alternative Biome States', *Science* **334**,
843 230-232.

844

845 Stocker, T. F.; Qin, D.; Plattner, G.-K.; Tignor, M.; Allen, S. K.; Boschung, J.; Nauels,
846 A.; Xia, Y.; Bex, V. & Midgley, P. M., ed. (2013), *IPCC, 2013: Climate Change 2013:
847 The Physical Science Basis. Contribution of Working Group I to the Fifth Assessment
848 Report of the Intergovernmental Panel on Climate Change*, Cambridge University
849 Press, Cambridge, United Kingdom and New York, NY, USA..

850

851 Svejcar, T.; Bates, J.; Angell, R. & Miller, R. (2003), 'The influence of precipitation
852 timing on the sagebrush steppe ecosystem. In: Guy, McPherson, Jake, Weltzin (Eds.),
853 Changing Precipitation Regimes & Terrestrial Ecosystems. University of Arizona Press,
854 Tucson, AZ 237pp.', .

855

856 Thomey, M. L.; Collins, S. L.; Vargas, R.; Johnson, J. E.; Brown, R. F.; Natvig, D. O. &
857 Friggens, M. T. (2011), 'Effect of precipitation variability on net primary production
858 and soil respiration in a Chihuahuan Desert grassland', *Global Change Biology* **17**,
859 1505-1515.

860

861 Trenberth, K. E.; Dai, A.; Rasmussen, R. M. & Parsons, D. B. (2003), 'The Changing
862 Character of Precipitation', *Bulletin of American Meterological Society* **84**, 1205-1217.

863

864 Vincens, A.; Garcin, Y. & Buchet, G. (2007), 'Influence of rainfall seasonality on
865 African lowland vegetation during the Late Quaternary: pollen evidence from Lake
866 Masoko, Tanzania', *Journal of Biogeography* **34**, 1274-1288.

867

868 Weltzin, J. F.; Loik, M. E.; Schwinning, S.; Williams, D. G.; Fay, P. A.; Haddad, B. M.;
869 Harte, J.; Huxman, T. E.; Knapp, A. K.; Lin, G.; Pockman, W. T.; Shaw, M. R.; Small,
870 E. E.; Smith, M. D.; Smith, S. D.; Tissue, D. T. & Zak, J. C. (2003), 'Assessing the
871 Response of Terrestrial Ecosystems to Potential Changes in Precipitation', *BioScience*
872 **53(10)**, 941-952.

873

874 Williams, C. A. & Albertson, J. D. (2006), 'Dynamical effects of the statistical
875 structure of annual rainfall on dryland vegetation', *Global Change Biology* **12**,
876 777-792.

877

878 Zhang, X.; Friedl, M. A.; Schaaf, C. B.; Strahler, A. H. & Liu, Z. (2005), 'Monitoring
879 the response of vegetation phenology to precipitation in Africa by coupling MODIS
880 and TRMM instruments', *Journal of Geophysical Research* **110**, **D12103**.

881

882 Zhang, Y.; Moran, M. S.; Nearing, M. A.; Campos, G. E. P.; Huete, A. R.; Buda, A. R.;
883 Bosch, D. D.; Gunter, S. A.; Kitchen, S. G.; McNab, W. H.; Morgan, J. A.; McClaran,
884 M. P.; Montoya, D. S.; Peters, D. P. & Starks, P. J. (2013), 'Extreme precipitation
885 patterns and reductions of terrestrial ecosystem production across biomes', *Journal of*
886 *Geophysical Research: Biogeosciences* **118**, 148-157.

887

Table 1. Summary of previous representative studies on assessing the impacts of rainfall characteristics (i.e. rainfall frequency, intensity and seasonality) on the structure and function of terrestrial ecosystem.

Focus: frequency (freq); intensity (int); seasonality (sea); variation (CV).

Methods: Field Experiments (Field); Remote Sensing (RS); Flux Tower (Flux).

Major Conclusion: increasing rainfall intensity (or decreasing frequency) has positive impacts (int+); increasing intensity (or decreasing frequency) has negative impacts (int-); increasing rainfall CV has positive impacts (CV+); increasing rainfall CV has negative impacts (CV-).

Focus	Methods	Spatial Scale	Time scale	MAP (mm/year)	Ecosystem type	Major Conclusion	Reference
freq; int	RS	Africa continent	intra-annual climatology	[0,3000]	Africa all	(int-) woody cover	Good and Caylor, 2011
freq; int	RS	US		[163,1227]	US	(int-) ANPP greatest in arid grassland (16%) and Mediterranean forest (20%) and less for mesic grassland and temperate forest (3%)	Zhang et al., 2013
freq; int	RS	Pan-tropics (35°N to 15°S)	inter-annual	[0,3000]	Tropical ecosystems	(CV+) wood cover in dry tropics; (CV-) wood cover in wet tropics	Holmgren et al., 2013
freq; int	RS	Northern China	intra-annual	[100,850]	temperate grassland and forests	(int-) NDVI for temperate grassland and broadleaf forests, not for coniferous forest	Fang et al., 2005
freq; int	Flux	Northern Hemisphere	intra-annual	[393±155,906±243]	shrubland and forest	(int-) GPP, RE and NEP	Ross et al., 2012
seas	RS	Africa continent	climatology	[0,3000]	Africa all	rainy season onset and offset controls vegetation growing season	Zhang et al., 2005
freq; int	Field	plot (Kansas, USA)	intra-annual	615	grassland	(int-) ANPP	Knapp et al., 2002

(fix MAP)							
freq; int (fix MAP)	Field	plot (Kansas, USA)	intra-annual	835	grassland	(int-) ANPP	Fay et al., 2003
increase seasonal rainfall	Field	plot(Texas, USA)	intra-annual	365	grassland	(int-) ANPP	Robertson et al., 2009
freq; int	Field	plot (Kansas, USA)	intra-annual	[320,830]	grassland	(int-)ANPP for MAP=830mm/yr; (int+)ANPP for MAP=320mm/yr	Heisler-White et al., 2009
freq; int	Field	plot(New Mexico, USA)	intra-annual	250	grassland	(int+) ANPP	Thomey et al., 2011
freq; int (fix MAP)	Field	Plot(Kansas, USA)	intra-annual	834	grassland	(int-) soil CO2 flux	Harper et al., 2005
freq; int (fix MAP)	Field	plot(Kruger National Park, South Africa)	intra-annual	544	sub-tropical savanna	(int+) wood growth; (int-) grass growth	Kulmatiski and Beard, 2013
sea (fix MAP)	Field	plot(Oregon, USA)	intra-annual	[140,530]	grassland	impact biomass and bare soil fraction	Bates et al., 2006; Svejcar et al., 2003
sea	Field						
freq; int; MAP	Field	plot(South Africa)	intra-annual	[538,798]	grassland	(int-) ANPP	Swemmer et al., 2007
MAP; sea	Field	plot(Spain)	intra-/inter-an nual	242	grassland	Mediterranean dryland ecosystem has more resilience for intra- and inter-annual changes in rainfall	Miranda et al., 2008

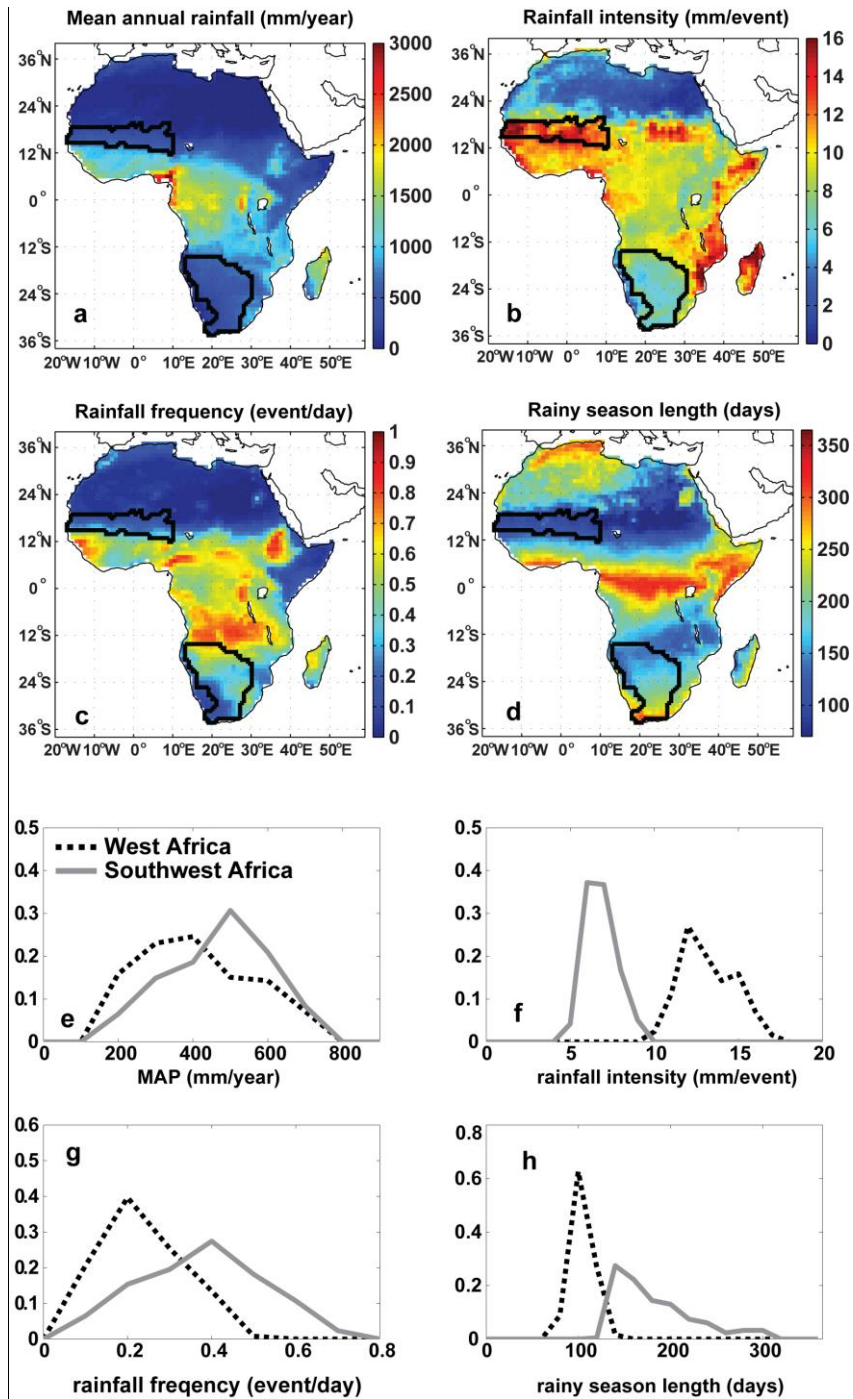


Figure 1. a-b: Spatial pattern of the rainfall characteristics in Africa: a-MAP; b-rainfall intensity; c-rainfall frequency; d-rainy season length. The black-line identified areas refer to two savanna regions in West and Southwest Africa. e-f: Normalized histograms of the rainfall characteristics in two savanna regions of West and Southwest Africa. e-MAP (bin width for the x-axis: 100 mm/year); f-rainfall intensity (bin width for the x-axis: 1 mm/event); g-rainfall frequency (bin width for the x-axis: 0.1 event/day); h-rainy season length (bin width for the x-axis: 20 days).

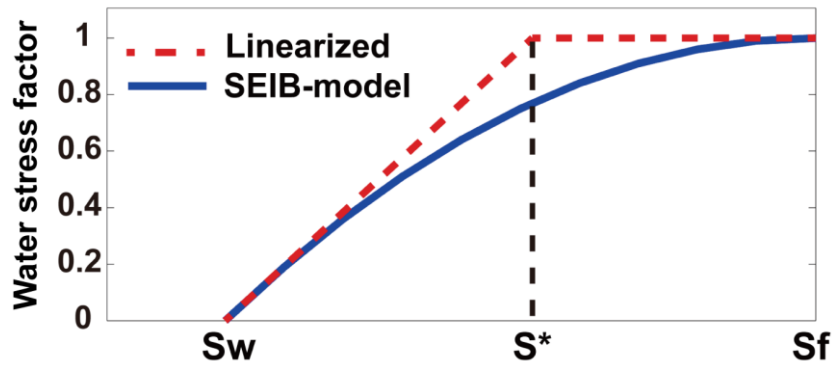


Figure 2. Schematic diagram of water stress factor ranging from 0 (most stressful) to 1 (no stress), which acts to reduce transpiration and carbon assimilation. The red dotted line is based on Porporato et al. (2001) with a reversed sign, and SEIB-DGVM has a nonlinear implementation (blue solid line, Sato and Ise, 2012).

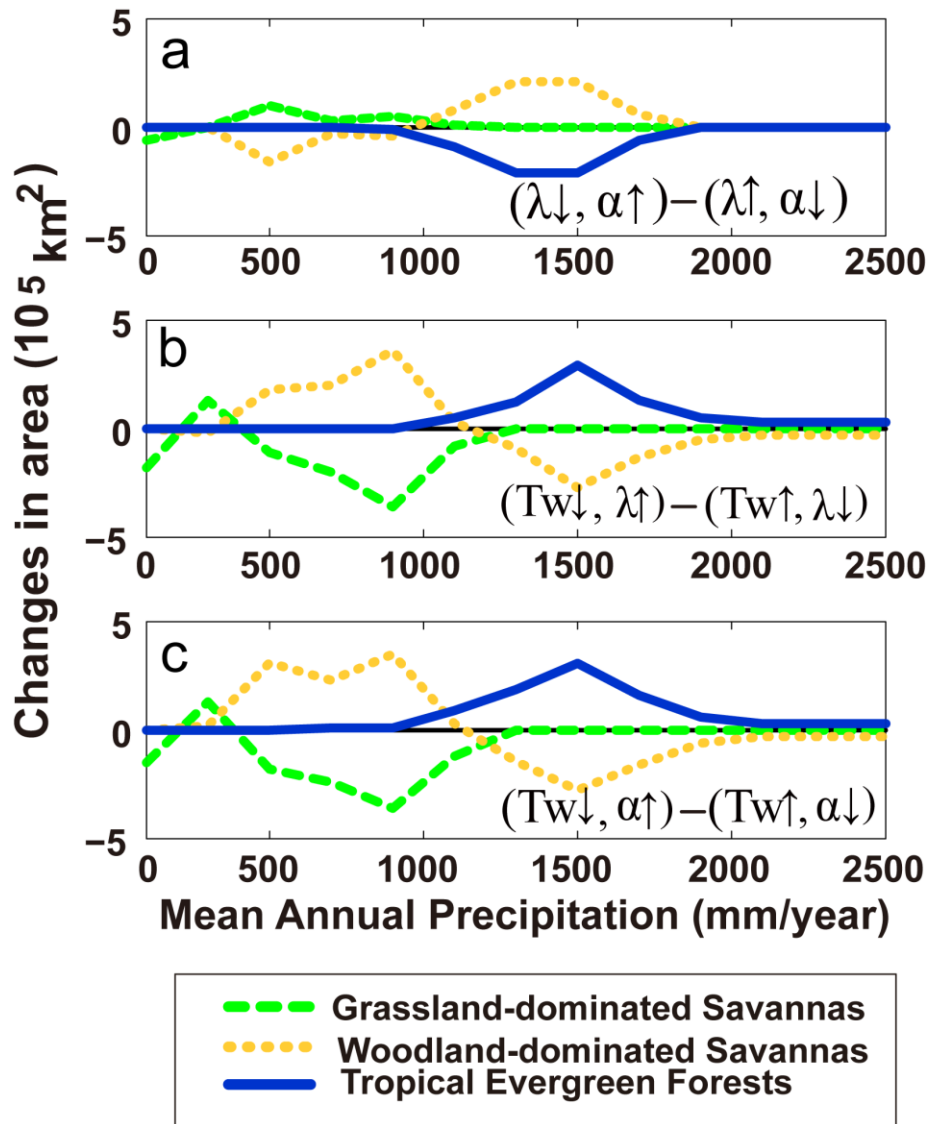


Figure 3. Differences in simulated dominated biomes in the three experiments (i.e. $S_{\lambda-\alpha}$, $S_{Tw-\lambda}$, $S_{Tw-\alpha}$).

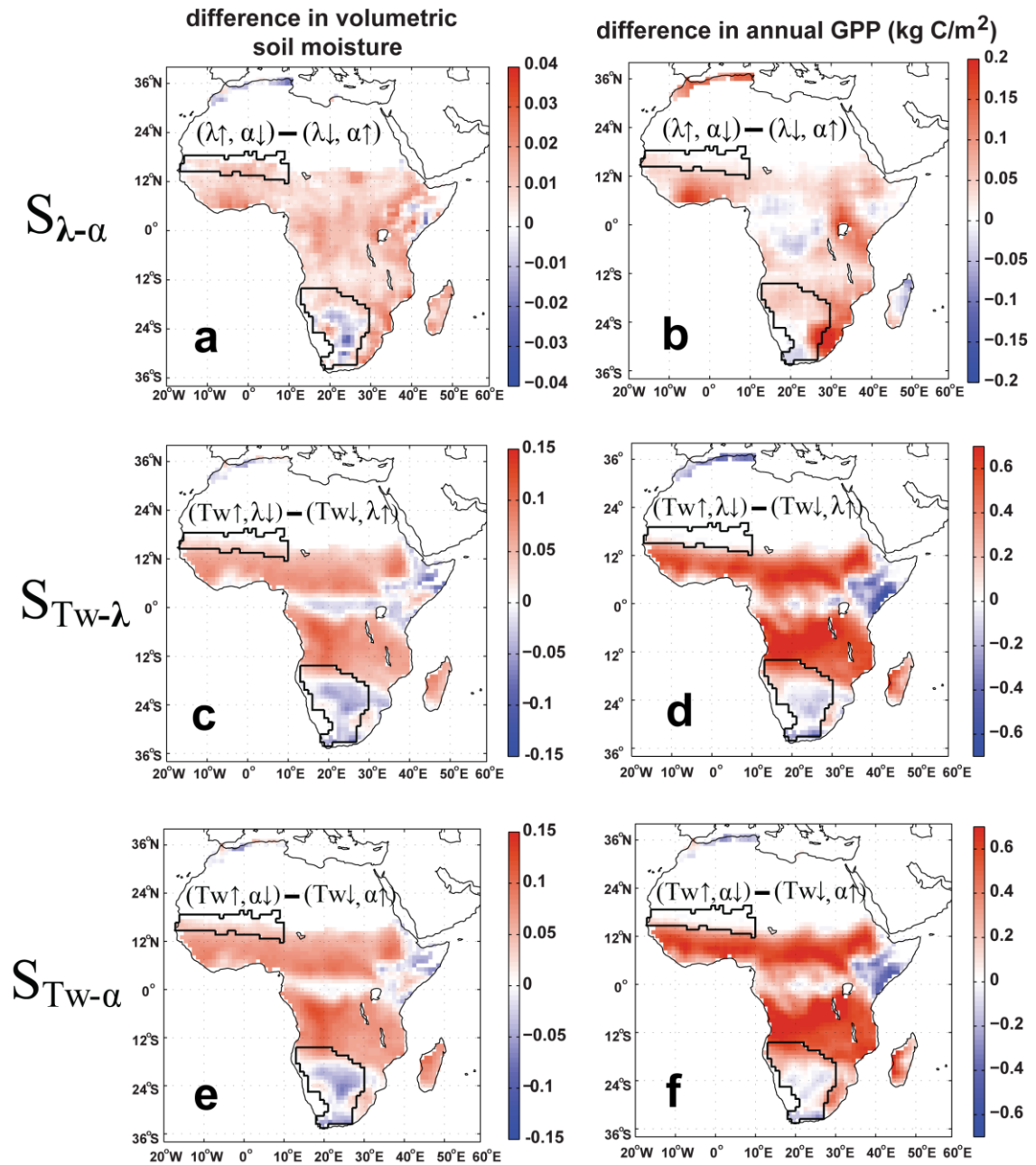


Figure 4. Simulated changes in annual mean soil moisture (0-500mm, first column) and annual mean GPP (second column) for different experiments. Please note that the scales of $S_{\lambda-\alpha}$ is much smaller than those of $S_{TW-\lambda}$ and $S_{TW-\alpha}$. The two areas with black boundaries in each panel are West African grassland and Southwest African grassland associated with Figure 1. The spatial patterns shown here are smoothed by 3*3 smoothing window from the raw data.

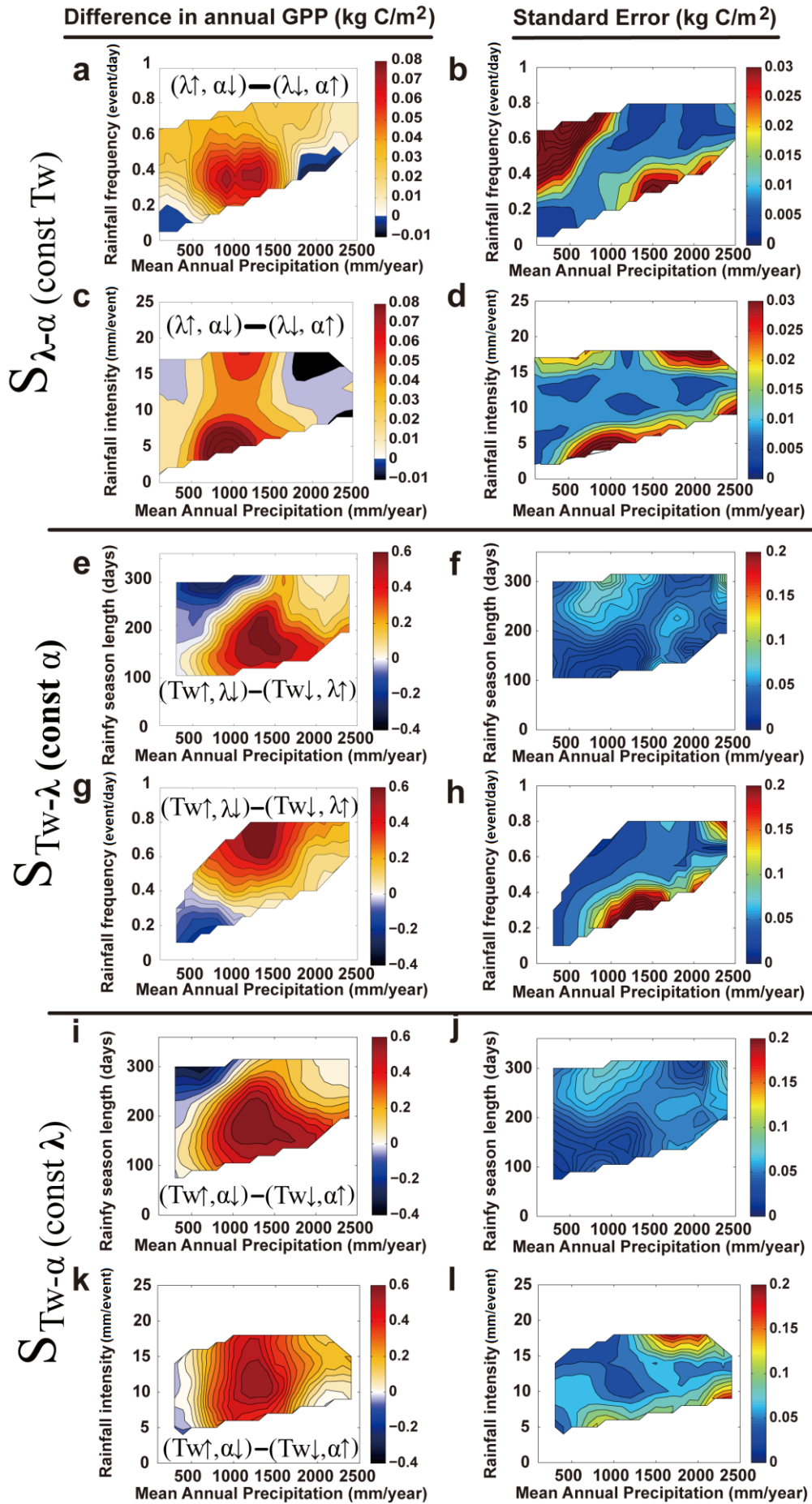


Figure 5. Differences in simulated annual GPP as a function of mean annual precipitation and one of the perturbed rainfall characteristics in all the three experiments (i.e. $S_{\lambda-a}$, $S_{TW-\lambda}$, S_{TW-a}) in the left column. The right column shows the correspondent standard errors (SE, calculated as $SE = \frac{\sigma}{\sqrt{n}}$, where σ refers to the standard deviation within each bin, n is the sample size in each bin, and n and σ are shown in Figure S4), with larger values associated with more uncertainties and requires more caution in interpretation. The contours are based on the binned values, with for each 100 mm/year in MAP, each 0.05 event/day in rainfall frequency, each 1 mm/event in rainfall intensity and each 15 day in rainy season length.

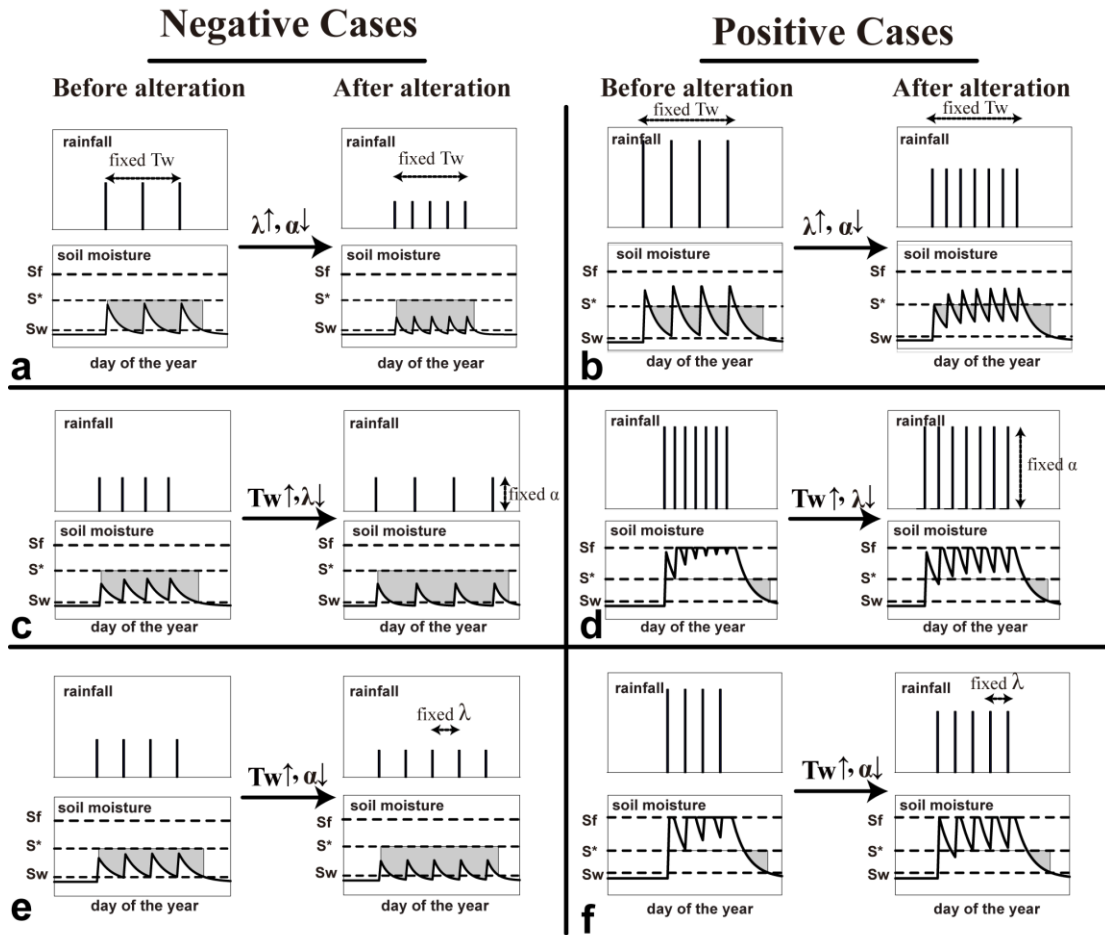


Figure 6. Illustrative time series for hydrological controls on plant root-zone soil moisture dynamics for all the experiments, and these illustrations are generalized based on the simulated time series from the experiments. Both negative and positive cases are shown, and cases with directly hydrological controls are shown (i.e. cloud-induced negative impacts in tropical forests are not shown). The cumulative shaded areas refer to “plant water stress” defined by Porporato et al. (2001).

Supplementary materials:

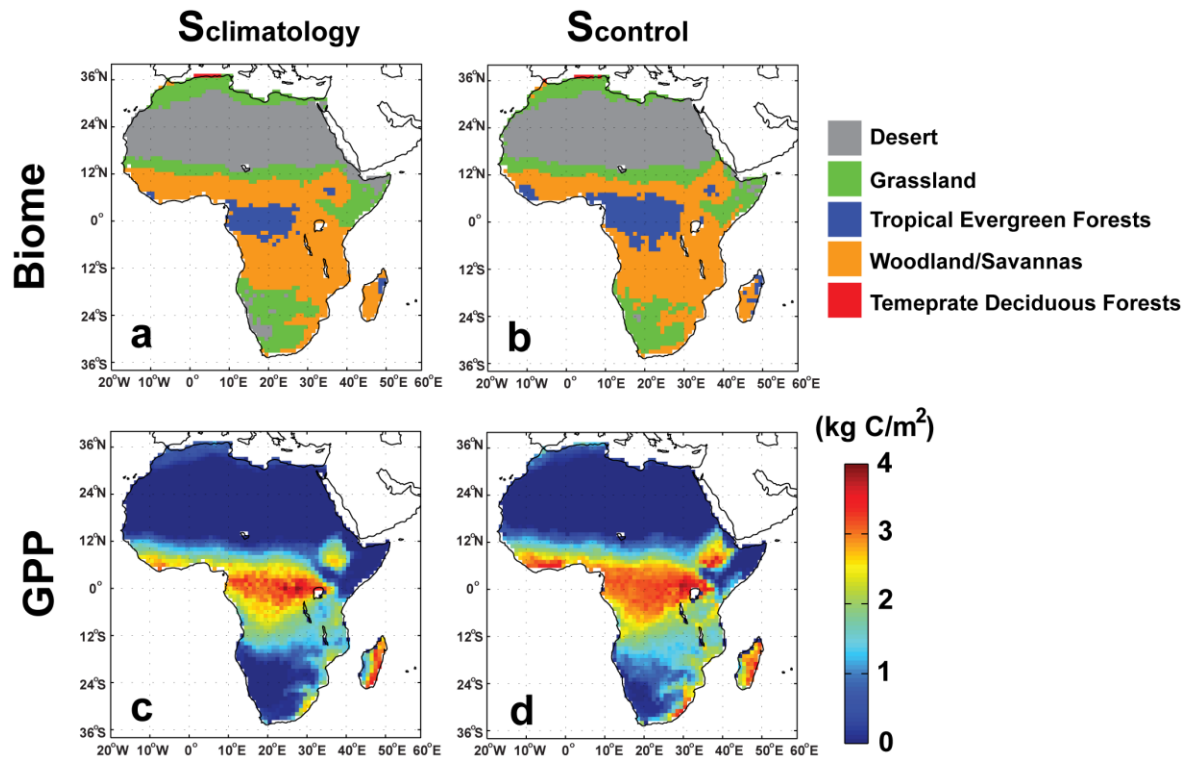


Figure S1. Comparison of biomes and annual GPP between $S_{climatology}$ and $S_{control}$ to test the validity of the synthetic weather generator. The biome definition follows Sato and Ise (2012).

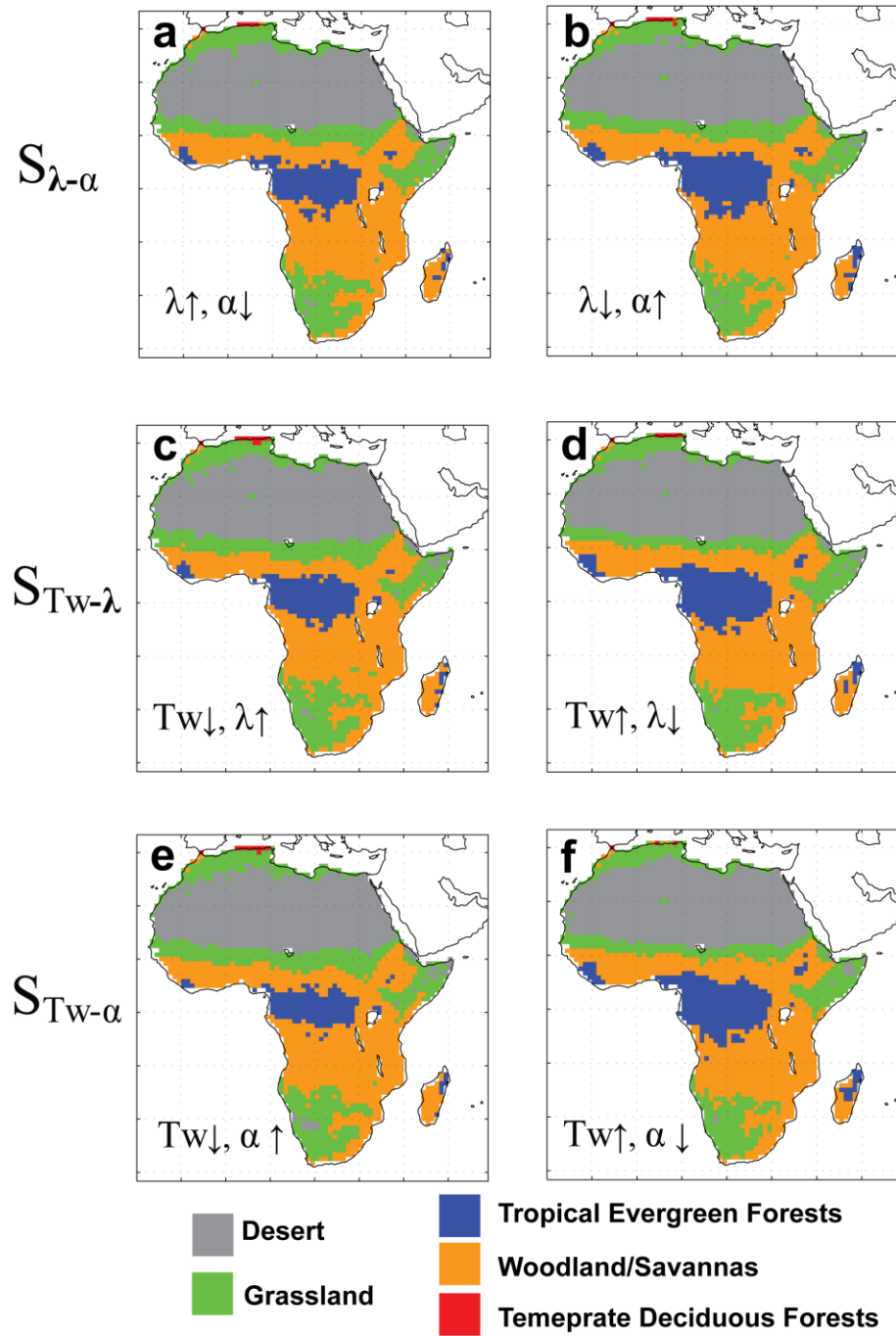


Figure S2. Simulated biomes for different experiments.

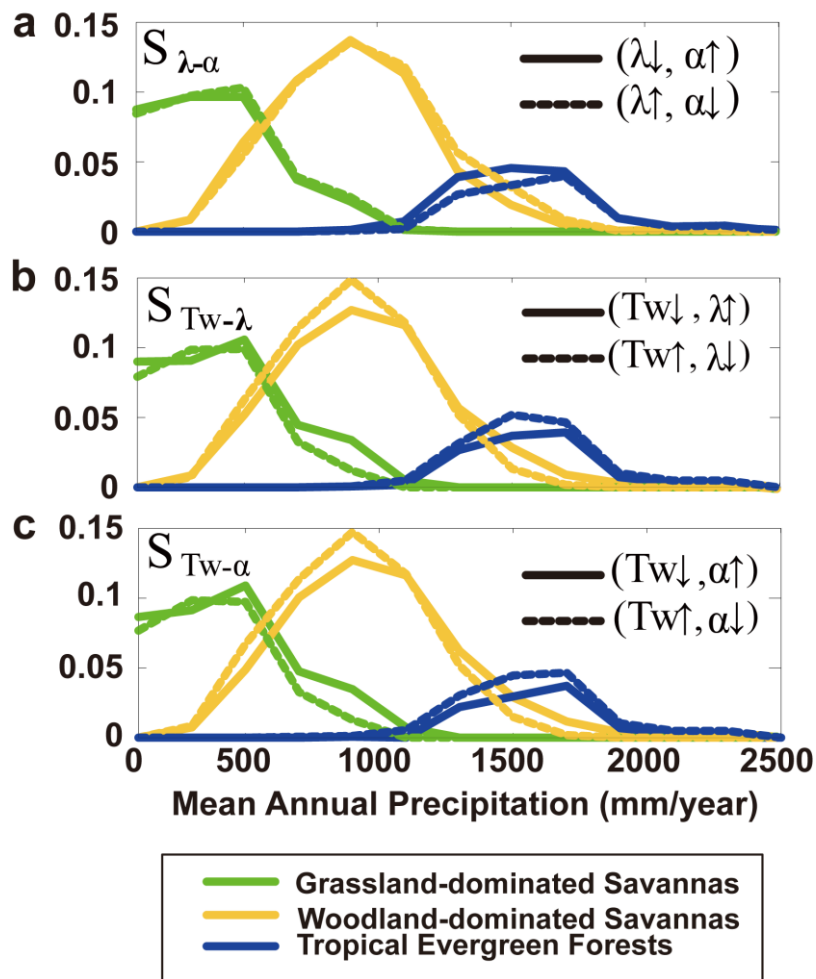


Figure S3. Normalized histograms of three simulated dominating biomes in the three experiments.

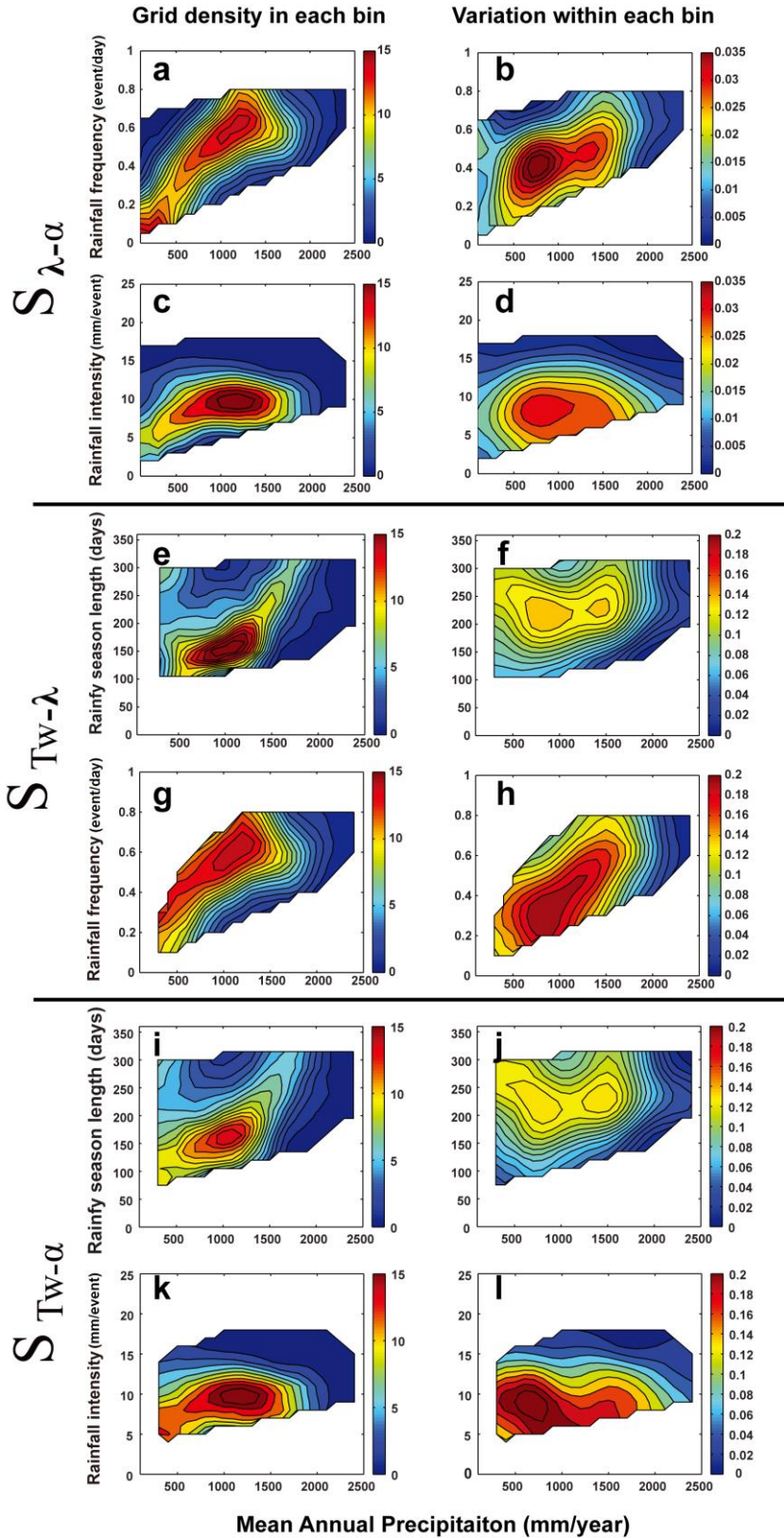


Figure S4. The sample size (n) in each bin (left column) and standard deviation (σ) in each bin (right column), corresponding to Figure 5. In Figure 5 right column, standard deviation (SE) is calculated as $SE = \frac{\sigma}{\sqrt{n}}$.